

Effect of Ethanol and Osmotic Stress on Receptor Conformation

REDUCED WATER ACTIVITY AMPLIFIES THE EFFECT OF ETHANOL ON METARHODOPSIN II FORMATION*

(Received for publication, September 2, 1999, and in revised form, October 25, 1999)

Drake C. Mitchell and Burton J. Litman‡

From the Section of Fluorescence Studies, Laboratory of Membrane Biophysics and Biochemistry,
National Institute on Alcohol Abuse and Alcoholism, National Institutes of Health, Rockville, Maryland 20853

The combined effects of ethanol and osmolytes on both the extent of formation of metarhodopsin II (MII), which binds and activates transducin, and on acyl chain packing were examined in rod outer segment disc membranes. The ethanol-induced increase in MII formation was amplified by the addition of neutral osmolytes. This enhancement was linear with osmolality. At 360 milliosmolar, the osmolality of human plasma, 50 mM ethanol was 2.7 times more potent than at 0 osmolality, demonstrating the importance of water activity in *in vitro* experiments dealing with ethanol potency. Ethanol disordered acyl chain packing, and increasing osmolality enhanced this acyl chain disordering. Prior osmotic stress data showed a release of 35 ± 2 water molecules upon MII formation. Ethanol increases this number to 49 water molecules, suggesting that ethanol replaces 15 additional water molecules upon MII formation. Amplification of ethanol effects on MII formation and acyl chain packing by osmolytes suggests that ethanol increases the equilibrium concentration of MII both by disordering acyl chain packing and by disrupting rhodopsin-water hydrogen bonds, demonstrating a direct effect of ethanol on rhodopsin. At physiologically relevant levels of osmolality and ethanol, about 90% of ethanol's effect is due to disordered acyl chain packing.

One of the proposed modes of action of ethanol on biological macromolecules and membranes involves the replacement of hydrogen-bonded water by ethanol (1, 2). Based on the hydrogen bonding capability of both water and ethanol, it is postulated that they compete for hydrogen bonding sites on the surface of lipids and proteins. Thus, this action of ethanol is equally applicable to mechanisms of ethanol action involving both lipid-mediated and direct protein interactions. The general importance of changes in hydration in enzyme activity is widely acknowledged (3, 4), but there is little detailed knowledge regarding how replacement of water by ethanol in specific protein-water hydrogen bonds might alter protein conformational equilibria or function. In addition, the physical properties of the surrounding phospholipid bilayer are known to modulate membrane function. Ethanol-induced changes in phospholipid hydrogen bonding have been observed to change acyl chain packing in pure lipid bilayers (5–7). Thus, the function of integral membrane receptors could be especially susceptible to the disruption of hydrogen-bonded water by ethanol.

Thorough examination of the interplay between ethanol and hydration in modulating membrane receptor function requires the ability to separately analyze the effects of ethanol on both protein structure and bilayer physical properties and to be able to correlate the observed changes. Previously, we examined the effects of ethanol (8) and a series of *n*-alkanols (9) on both the MI¹-MII conformational equilibrium and acyl chain packing in the surrounding bilayer. In the present work, the effects of ethanol on the MI-MII equilibrium and acyl chain packing are reexamined as a function of osmotic stress.

The osmotic stress protocol (10) is an established method for determining changes in the number of bound water molecules associated with a specific enzymatic process. This experimental strategy is based on the fact that the effect of a neutral osmolyte on the water activity of aqueous compartments in equilibrium with a protein depends on the degree to which it is excluded from the protein-associated water. Osmolyte inaccessibility is determined by the protein topology and the size of the osmolyte (11). The result is that by reducing the activity of water, the presence of an osmotically active osmolyte inhibits protein conformational changes in which there is a net uptake of water and favors processes in which a protein releases water to the bulk aqueous medium. Osmolytes, which are so small that they are not excluded from any clefts or pockets on the protein surface, will not be osmotically active (12). Recently, we employed this technique to show that the MI to MII transition of photoactivated rhodopsin is dependent upon water activity, with the MII conformation binding 35 ± 2 fewer water molecules than MI (13).

Rhodopsin resides in the retinal ROS disc membrane, where it represents about 95% of the integral membrane protein. About half of its mass is within the lipid bilayer, while the other half makes up the hydrophilic loops, connecting the α -helices. The detailed structural information obtained recently for both the loops (14) and the transmembrane helices (15, 16) makes rhodopsin the most well characterized member of the G protein-coupled receptor superfamily. Within a few milliseconds of light absorption, a metastable equilibrium is established between MII, the conformation which binds and activates transducin (17), and its inactive precursor, MI (18). The MI-to-MII conformational change is the principal conformational change of photolyzed rhodopsin, and many details of this structural change have been determined (19), including changes in the hydrogen bonding of internal water molecules (20, 21). Previous studies have determined the sensitivity of MII formation with respect to both bilayer composition and phospholipid bilayer acyl chain packing (22–24). The available structural information for rhodopsin coupled with its central role in visual transduction and its relationship to neurotrans-

* The costs of publication of this article were defrayed in part by the payment of page charges. This article must therefore be hereby marked "advertisement" in accordance with 18 U.S.C. Section 1734 solely to indicate this fact.

‡ To whom correspondence should be addressed: Park Bldg., Room 158, 12420 Parklawn Dr., Rockville, MD 20852. Tel.: 301-594-3608; Fax: 301-594-0035; E-mail: litman@helix.nih.gov.

¹ The abbreviations used are: MI, metarhodopsin I; MII, metarhodopsin II; ROS, rod outer segment; DPH, 1,6-diphenyl-1,3,5-hexatriene.

mitter receptors make rhodopsin an ideal receptor on which to study the interplay between hydration and ethanol.

Ethanol and osmotic stress have opposite effects on acyl chain packing. The ability of ethanol to disorder phospholipid acyl chain packing has been measured in a large number of natural and artificial membranes by several techniques (8, 9, 25). In contrast, osmotic stress, or lowered water activity, leads to increased phospholipid acyl chain packing with a concomitant reduction in bilayer free volume (13, 26). A complicating factor in most ethanol experiments, which obscures their relevance to *in vivo* effects, is that they are generally performed on dilute aqueous suspensions of membranes or artificial vesicles. In such experiments, the potential for *in vivo* osmotic conditions to alter water activity and thereby change the effect of ethanol on membranes is left in question. In this study, we examined the combined effects of ethanol and osmotic stress on both the activating conformational change of the G protein-coupled receptor rhodopsin (*i.e.* the formation of MII) and on acyl chain packing of the ROS disc membrane.

EXPERIMENTAL PROCEDURES

Sample Preparation—Intact ROS disks were prepared from frozen bovine retinas as described previously (27). Stachyose was purchased from Sigma, and DPH was purchased from Molecular Probes, Inc. (Eugene, OR). Samples for all studies (8 μM rhodopsin for all absorbance measurements, 1.2 μM rhodopsin for fluorescence measurements) were prepared in a low ionic strength buffer (10 mM HEPES, 50 μM diethylenetriaminepentaacetic acid, pH 7.5) with the required osmolyte. Osmolyte-containing samples were then put through 10 freeze-thaw cycles to ensure that the osmolyte had equilibrated across the membrane and then were extruded through a 0.2- μm pore filter 10 times to reduce scattered light. All procedures were carried out under argon in a glove box to minimize oxidation of the polyunsaturated acyl chains of the ROS disc membrane. The osmolality of all solutions was determined with a Wescor Vapro 5520 vapor pressure osmometer.

Equilibrium Absorbance Measurements—Absorbance spectra of MI-MII equilibrium mixtures ~ 3 s following a flash that bleached 15–20% of the rhodopsin were acquired with a Hewlett-Packard 8452A diode array spectrophotometer (0.2-s measurements yielded $<0.3\%$ bleach by measuring beam) (28). Individual MI and MII bands were resolved by using nonlinear least squares to fit the sum of two asymmetric Gaussian absorbance bands to difference spectra that had been corrected for the presence of unbleached rhodopsin (28). The equilibrium constant for the MI to MII conversion is defined by $K_{\text{eq}} = [\text{MII}]/[\text{MI}]$. In determining the effect of neutral osmolytes, the ethanol-free osmolyte solution served as the control; thus, when examining effects of the osmolytes on the ethanol-induced MII formation, the solution osmolality does not include the contribution due to ethanol. The change in free energy, $\Delta(\Delta G)$, for the MI-MII equilibrium due to the presence of ethanol was calculated according to the following.

$$\Delta(\Delta G) = \Delta G_{\text{ethanol}} - \Delta G_{\text{ethanol-free control}} \quad (1)$$

The effect of osmotic stress on the MI-MII equilibrium was analyzed using established thermodynamic relationships (10). The change in the number of water molecules in osmolyte-inaccessible regions, ΔN_w , is given by the slope of line relating $\ln(K_{\text{eq}})$ and the osmolyte concentration as follows.

$$\ln(K_{\text{eq}}) = -\Delta N_w \times \frac{[\text{osmolal}]}{55.6} \quad (2)$$

Fluorescence Measurements and Analysis—Fluorescence lifetime and differential polarization measurements were performed with an ISS K2 multifrequency cross-correlation phase fluorometer with excitation provided by an Innova 307 Argon ion laser (Coherent). Lifetime and differential polarization data were acquired using 15 modulation frequencies, logarithmically spaced from 5 to 250 MHz. Scattered excitation light was removed from the emission beam by a 390-nm high pass filter. All lifetime measurements were made with the emission polarizer at 54.7° relative to the vertically polarized excitation beam and with 1,4-bis(5-phenyloxazol-2-yl)benzene in absolute ethanol in the reference cuvette. For each differential polarization measurement, the instrumental polarization factors were measured and found to be between 1 and 1.05, and the appropriate correction factor was applied. At each

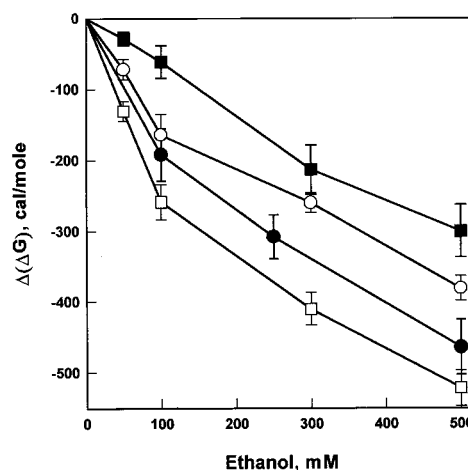


FIG. 1. Neutral osmolyte enhancement of the effects of ethanol on $\Delta(\Delta G)$ for the MI to MII transition. $\Delta(\Delta G)$ was calculated according to $\Delta(\Delta G) = \Delta G_{\text{ethanol}} - \Delta G_{\text{ethanol-free control}}$ (Equation 1). Solutions are 0.3 M sucrose (○), 0.4 M stachyose (●), 1.0 M sucrose (□), and control with no osmolyte agent (■).

frequency, data were accumulated until the S.D. values of the phase and modulation ratio were below 0.2° and 0.004, respectively, and these values were used as the S.D. for the measured phases and modulation ratios in all subsequent analysis. Both total intensity decay and differential polarization measurements were repeated a minimum of three times.

Measured polarization-dependent differential phases and modulation ratios for each sample were combined with the measured total intensity decay to yield the anisotropy decay, $r(t)$. All anisotropy decay data were analyzed using the Brownian rotational diffusion model as described previously (29). The results of the Brownian rotational diffusion model-based analysis were interpreted in terms of an angular distribution function, $f(\theta)$, which is symmetric about $\theta = \pi/2$ (29). The extent to which the equilibrium orientational freedom of DPH is restricted by the phospholipid acyl chains was quantified using the parameter f_v (30), which is defined as follows.

$$f_v = 1/(2f(\theta)_{\text{max}}) \quad (3)$$

All measurements were performed at 20°C , and all data analysis were performed with NONLIN (31), with all subroutines specifying the fitting functions written by the authors. Confidence intervals corresponding to 1 S.D. were obtained by NONLIN for both fitting variables and derived parameters.

Bilayer Correction Factor to $\Delta(\Delta G)$ —The bilayer correction to account for the effect of altered phospholipid acyl chain packing on $\Delta(\Delta G)$ was calculated using the known relationship between $\Delta(\Delta G)$ and f_v induced by varying independently both ethanol concentration and osmotic pressure. These relationships allowed the determination of $(\partial\Delta G/\partial f_{v,\text{EtOH}})$ and $(\partial\Delta G/\partial f_{v,\text{Os}})$, respectively. Specifically, the measured changes in f_v due to the presence of osmolytes were subtracted from the observed changes in f_v due to the presence of both osmolyte and ethanol to obtain the value of $\Delta f_{v,\text{EtOH}}$. This allowed the inclusion of the enhanced effect of ethanol induced by the presence of the osmolyte. $\Delta(\Delta G)_{\text{bilayer}}$ was calculated according to Equation 4.

$$\Delta(\Delta G)_{\text{bilayer}} = \Delta f_{v,\text{Os}}(\partial\Delta G/\partial f_{v,\text{Os}}) + \Delta f_{v,\text{EtOH}}(\partial\Delta G/\partial f_{v,\text{EtOH}}) \quad (4)$$

RESULTS

Effect of Ethanol on MI-MII Equilibrium in the Presence of Osmolytes—Previous studies showed that both neutral osmolytes (13) and ethanol (8, 9) shift the MI-MII equilibrium toward MII. In order to compare the combined effect of ethanol and osmolytes on the MI-MII equilibrium, the observed shifts in K_{eq} were converted to differences in the change in free energy in the presence and absence of ethanol, $\Delta(\Delta G)$ (Equation 1). In the absence of osmolyte, increasing the ethanol concentration made $\Delta(\Delta G)$ more negative (*i.e.* ethanol shifted the MI-MII equilibrium toward MII), as shown by the control curve for 0 sucrose in Fig. 1. The effect of ethanol was amplified by the presence of neutral osmolyte, as shown by the curves for

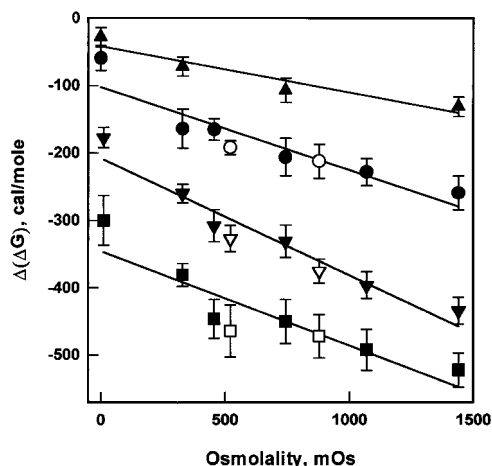


FIG. 2. Osmolality enhances the effect of ethanol on $\Delta(\Delta G)$ for the MI to MII transition. Filled symbols represent sucrose solutions; open symbols represent stachyose solutions. \blacktriangle , 50 mM ethanol; \bullet , 100 mM ethanol; \blacktriangledown , 300 mM ethanol; \blacksquare , 500 mM ethanol.

sucrose and stachyose (Fig. 1). Increasing osmolyte concentration reduces water activity. The effect of decreasing water activity on the efficacy of ethanol is demonstrated by plotting $\Delta(\Delta G)$ due to ethanol as a function of increasing osmolality for four different ethanol concentrations, Fig. 2. The effect of 50, 100, 300, and 500 mM ethanol on the MI-MII equilibrium increased approximately linearly with increasing osmolality. Solution osmolality was varied with sucrose, except for where shown by the open symbols, which correspond to stachyose solutions. An earlier investigation of the effects of osmotic stress showed that the influence of sucrose and stachyose on the MI-MII equilibrium is equivalent at the same osmolal concentration (13). The clear trend of decreasing $\Delta(\Delta G)$ with increasing osmolality for both sucrose and stachyose (Fig. 2) demonstrates that at a given ethanol concentration, reduced water activity enhances the ability of ethanol to promote the formation of the MII conformation.

Effect of Osmolytes and Ethanol on DPH Fluorescence—The effect of solute osmolality on ethanol-induced phospholipid acyl chain disordering was assessed by analyzing the fluorescence lifetime and anisotropy decay of DPH under the same osmolyte and ethanol conditions used to study the MI-MII equilibrium. The DPH fluorescence lifetime was well characterized by a decay scheme consisting of a Lorentzian distribution plus two discrete components, which produced values of χ^2 between 0.9 and 2.5. The lifetimes of the two discrete components ranged from 2.2 to 1.4 ns and from 0.27 to 0.22 ns, respectively, and together they accounted for 10–15% of the decay under all conditions. The high concentration of rhodopsin in the ROS disc membrane (1 rhodopsin per 75 phospholipids) results in substantial quenching of the DPH fluorescence due to energy transfer to the retinal chromophore. This quenching of DPH fluorescence by retinal is the probable source of the two short lifetime components. In the absence of ethanol, the center of the Lorentzian distribution ranged from 9.1 to 9.5 ns under all osmolyte conditions, and the maximum change was seen in 500 mM ethanol where this value was reduced by about 0.3 ns for all osmolyte conditions.

The effect of ethanol on the decay of fluorescence anisotropy, $r(t)$, was also increased by the addition of osmolyte. The Brownian rotational diffusion model characterizes $r(t)$ in terms of the equilibrium orientational distribution of the probe, $f(\theta)$, and the rotational diffusion coefficient, D_{\perp} (29). For a free-tumbling probe like DPH, $f(\theta)$ is especially informative regarding acyl chain packing, because $f(\theta)$ consists of the set of angular orien-

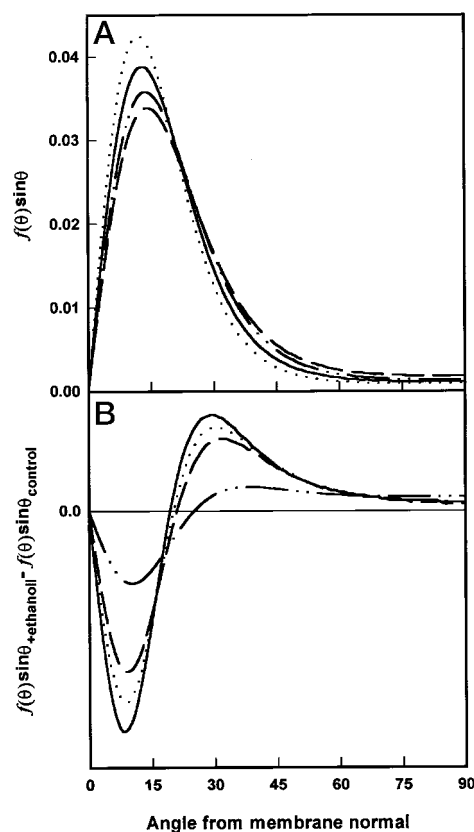


FIG. 3. A, the effects of neutral solutes and ethanol, alone or in combination, on the DPH orientational probability distribution, $f(\theta) \sin\theta$. Dashed and dotted line, 0 osmolyte, 0 ethanol control; dashed line, 0 osmolyte, 500 mM ethanol; dotted line, 1440 mOsm sucrose, 0 ethanol; solid line, 1440 mOsm sucrose, 500 mM ethanol. B, difference curves showing how the change in $f(\theta) \sin\theta$ due to 100 mM ethanol is increased by osmolality. Curves were obtained by subtracting $f(\theta) \sin\theta$ obtained with the specified solute osmolality in the absence of ethanol from the distribution obtained in the presence of 100 mM ethanol at the corresponding solute osmolality. Regions below the zero line correspond to the range of angular orientations where ethanol reduces the DPH orientational probability distribution, while regions above the zero line correspond to angular orientations where ethanol increases the DPH orientational probability distribution. Dashed and dotted line, 0 mOsm; dashed line, 330 mOsm sucrose; dotted line, 740 mOsm sucrose; solid line, 1440 mOsm sucrose.

tations that DPH is allowed to adopt within the confines of the ensemble packing of the phospholipid acyl chains. The shape of the orientation probability distribution, $f(\theta) \sin\theta$, provides information about relative acyl chain packing density at different depths in the bilayer, and the extent of overlap of $f(\theta) \sin\theta$ with a random orientational distribution indicates the degree of overall ordering of DPH by the acyl chains. Individually, neutral osmolytes and ethanol had large and opposite effects on $f(\theta) \sin\theta$, as shown by comparing the curve for 0 osmolyte, 0 ethanol with those for 0 osmolyte, 500 mM ethanol, and 1440 mOsm sucrose, 0 ethanol in Fig. 3A. Osmolytes narrowed the unimodal distribution centered about the membrane normal, while ethanol broadened the distribution, and this broadening was enhanced by the presence of osmolyte, as shown by the curve for 1440 mOsm, 500 mM ethanol. However, the disordering effect of ethanol was not strong enough to fully reverse the ordering effect of the osmolyte. An example of the manner in which reduced water activity enhanced the ethanol-induced changes in $f(\theta) \sin\theta$ is shown by the difference curves in Fig. 3B, which demonstrate the net effect on $f(\theta) \sin\theta$ of 100 mM ethanol for four different solute osmolalities. The curves in Fig. 3B were obtained by subtracting $f(\theta) \sin\theta$ obtained with the specified

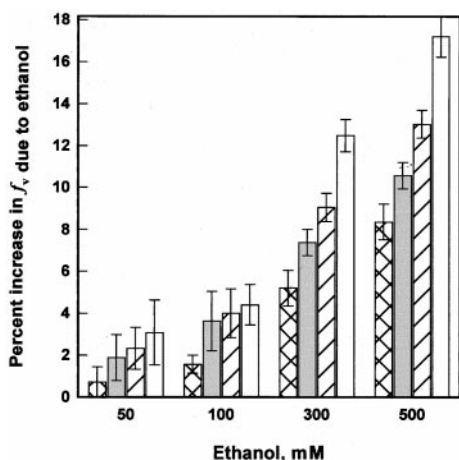


FIG. 4. Combined effects of ethanol and solute osmolality on the parameter f_v in terms of percentage increase induced by ethanol at each osmolality. Cross-hatched bars, 0 mOsm; gray bars, 330 mOsm sucrose; diagonally striped bars, 730 mOsm sucrose; white bars, 1440 mOsm sucrose.

solute osmolality in the absence of ethanol from the distribution obtained in the presence of 100 mM ethanol at the corresponding solute osmolality. Areas below the zero line in Fig. 3B correspond to angular orientations from which the DPH is excluded in the presence of ethanol, and areas above the zero line denote angular orientations that are preferentially allowed by the bilayer in the presence of ethanol. Ethanol enhanced DPH orientations greater than $\sim 20^\circ$ from the membrane normal, and an increase in the concentration of added osmolyte amplified this effect. As the osmolyte concentration was increased, 100 mM ethanol progressively broadened the probability distribution centered about the membrane normal.

A convenient, quantitative means of comparing different orientational probability distributions is the parameter f_v (Equation 3), which is proportional to the overlap of $f(\theta) \sin\theta$ for a given sample and $f(\theta) \sin\theta$ of a random distribution (29), and thus is a measure of ensemble acyl chain order. A higher value of f_v indicates an orientational distribution that is more like a random distribution. The separate effects of ethanol and the reduced water activity caused by increased osmolality on f_v are antagonistic, with ethanol causing an increase in f_v (8, 9), while in the absence of ethanol, reduced water activity lowers f_v (13). However, the net result of these two factors acting simultaneously is that the effect of ethanol is amplified by reduced water activity, as shown in Fig. 4. At 330 mOsm, the effect of 50 and 100 mM ethanol is increased by about a factor of 2.5, relative to dilute buffer conditions.

Previous investigations demonstrated a direct correlation between the MI-MII equilibrium constant and f_v , when both parameters are altered by changes in temperature or bilayer cholesterol content (22–24). In order to examine the relationship between ethanol-induced changes in acyl chain packing and in the MI-MII equilibrium, values of $\Delta(\Delta G)$ and Δf_v due to ethanol were plotted against each other for each solute osmolality (Fig. 5). As the concentration of ethanol increases at each osmolality, the $\Delta(\Delta G)$ values become more negative and the Δf_v values become larger. For 0 mOsm, the correlation is linear; however, as the osmolality increases, this relationship becomes increasingly nonlinear. This nonlinearity suggests that $\Delta(\Delta G)$ is being influenced by some factor in addition to the ethanol-induced changes in bilayer acyl chain order, reflected in the increase in f_v .

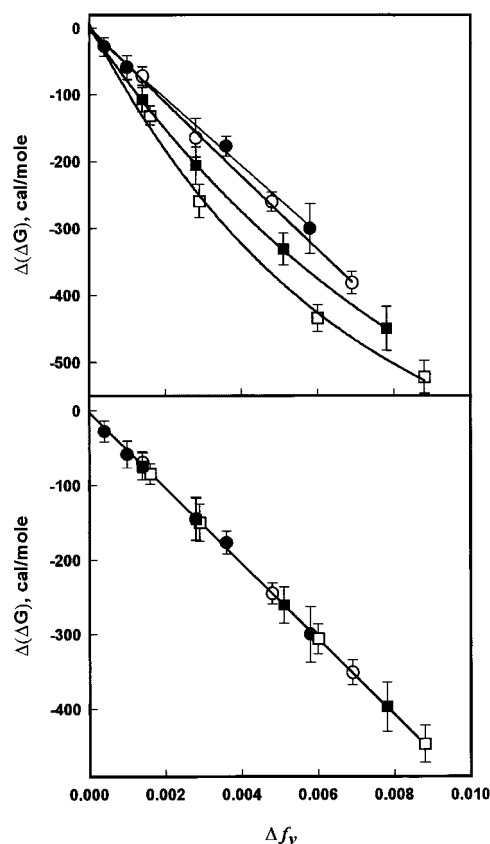


FIG. 5. Correlation between ethanol-induced changes in ΔG and f_v at four different osmolalities. $\Delta f_v = f_v(\text{with ethanol}) - f_v(\text{ethanol-free control})$. A, observed values of $\Delta(\Delta G)$. B, values of $\Delta(\Delta G)$ corrected for the effects of ethanol and osmolyte on acyl chain packing, as described under "Experimental Procedures." In order of decreasing value of $\Delta(\Delta G)$, the symbols within each group correspond to 50, 100, 300, and 500 mM ethanol. ●, 0 mOsm; ○, 330 mOsm sucrose; ■, 740 mOsm sucrose; □, 1440 mOsm sucrose.

DISCUSSION

One of the important issues in *in vitro* studies of the mechanism(s) of ethanol's action on biological systems is the biologically relevant range of concentrations of ethanol (32). The present data can be used to address this issue by considering the osmolality-induced increase in ethanol potency observed when measurements made in the presence of a neutral osmolyte, at the osmolality of human plasma, are compared with the results obtained for ethanol at 0 osmolality. For example, Fig. 1 shows that 250 mM ethanol in 400 mM stachyose produces a $\Delta(\Delta G)$ of -300 cal/mol, while in the absence of osmolyte 500 mM ethanol is required to produce this value of $\Delta(\Delta G)$. The relationship between osmolality and the ethanol dose that is required for an equivalent effect at 0 osmolality is very linear for all of the osmolyte-containing solutions. Therefore, all of the data can be used to determine the effects of 50 and 100 mM ethanol on the MI to MII conformation change at the osmolality of human plasma, 360 mOsm. At this osmolality, 50 mM ethanol would be equivalent to 134 ± 20 mM at 0 osmolality, and 100 mM would be equivalent to 291 ± 12 mM. Thus, at the osmolality of human plasma, the potency of ethanol in the 50–100 mM range is increased by a factor of 2.7–2.9. Using this potency factor, the substantial changes observed at 0 osmolality with 50 and 100 mM ethanol would be observed at about 18 and 36 mM ethanol, respectively, at the osmolality of plasma.

The sensitivity of rhodopsin to changes in membrane composition and phospholipid acyl chain packing is well documented. Hence, it is reasonable to question whether the os-

molyte enhancement of the effect of ethanol on MII formation arises through some direct interaction of ethanol on rhodopsin or via a lipid-mediated process induced by increased binding of ethanol to the bilayer. Earlier studies demonstrate that factors that increase K_{eq} (e.g. higher temperature (22, 23, 24), increased phospholipid acyl chain unsaturation (23, 24), decreased bilayer cholesterol (22, 23)) also increase f_v , and changes in K_{eq} and f_v are linearly related. Ethanol-induced changes in $\Delta(\Delta G)$ and Δf_v are also linearly related in the absence of osmolyte, as shown in Fig. 5A. Fig. 4 shows that osmotic stress increases the ability of ethanol to loosen acyl chain packing, as shown by the greater percentage increases in f_v with increasing osmolality for all ethanol concentrations. If all of the ethanol-induced increase in MII formation is due to ethanol-induced changes in acyl chain packing, then the correlation lines in Fig. 5A would be coincident, and increasing osmolality would simply shift each group of points to higher values of Δf_v and more negative values of $\Delta(\Delta G)$. However, marked nonlinearity and deviations from the 0 osmolyte $\Delta(\Delta G)$ versus Δf_v correlation line are observed.

A possible interpretation of the nonlinearity seen in Fig. 5A is that it reflects an osmotic stress-dependent component to the enhancement of MII formation by ethanol, which acts in addition to the effect of ethanol on acyl chain packing. This interpretation is consistent with the idea that the basic mechanism whereby ethanol reduces acyl chain packing order in the core of the bilayer is unaltered by osmotic stress. This basic mechanism involves hydrogen bonding to the phospholipid carbonyl oxygen, resulting in increased average phospholipid head group spacing, which induces acyl chain disorder (33). The increased ability of ethanol to disorder acyl chain packing with reduced water activity (Figs. 4 and 5A) is probably due to its enhanced competition with water for this hydrogen bonding site at reduced water activity. The data in Fig. 5A acquired in the absence of osmotic stress, the 0 osmolyte data, represent the correlation between ethanol-induced changes in the MI-MII equilibrium and ethanol-induced changes in acyl chain packing. It is similar to the linear correlation between these two parameters when both are altered by variation in temperature or bilayer cholesterol content (22–24). The 0 osmolyte, $\Delta(\Delta G)$ versus Δf_v correlation line can be interpreted as representing the susceptibility of the MI-MII equilibrium to changes in acyl chain packing due to ethanol. This allows the $\Delta(\Delta G)$ versus Δf_v correlation to be used to identify the fraction of the magnified effects of ethanol on K_{eq} , which are due to changes in acyl chain packing. The slope of the 0 osmolyte, $\Delta(\Delta G)$ versus Δf_v correlation line indicates that an ethanol-induced increment in f_v of 0.01 will decrease ΔG by 510 cal/mol. By using this relationship, we can examine to what extent the ethanol-induced decreases in ΔG under osmotic stress are attributable to changes in acyl chain packing and thus mediated by the membrane. The extra $\Delta(\Delta G)$ component under various osmotic conditions corresponds to the deviation of those points on the $\Delta(\Delta G)$ axis from the 0 osmolyte correlation line in Fig. 5A. The corrected $\Delta(\Delta G)$ values are shown in Fig. 5B. The results of this analysis show that under all osmotic conditions and ethanol concentrations examined, the effect of ethanol on ΔG is greater than what would be expected from the ethanol-induced increases in f_v , as summarized in Fig. 6. The bars in Fig. 6 represent the fraction of ethanol's effect on the MI-MII equilibrium that exceeds the membrane-mediated effect of ethanol. We would assign this component of $\Delta(\Delta G)$ to a direct effect of ethanol on rhodopsin. Near physiological osmolality, at 330 mOsm, the effect of 50 mM ethanol on the MI-MII equilibrium is $\sim 90\%$ due to changes in acyl chain packing and $\sim 10\%$ due to a direct effect of ethanol on rhodopsin (Fig. 6). At all concentrations of ethanol, the

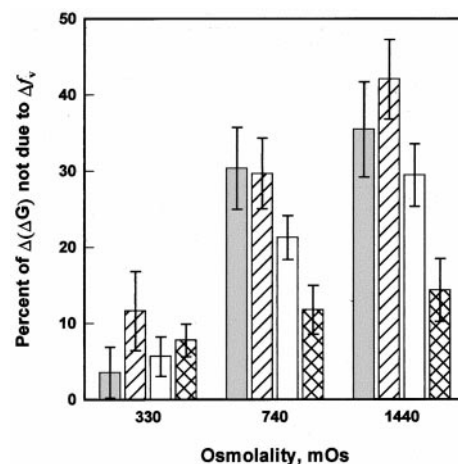


FIG. 6. Percentage of ethanol-induced $\Delta(\Delta G)$ that is in excess of the decrease in ΔG predicted by the $\Delta(\Delta G) - \Delta f_v$ correlation line in Fig. 5B for 50 mM ethanol (gray bars), 100 mM ethanol (diagonally striped bars), 300 mM ethanol (white bars), and 500 mM ethanol (cross-hatched bars).

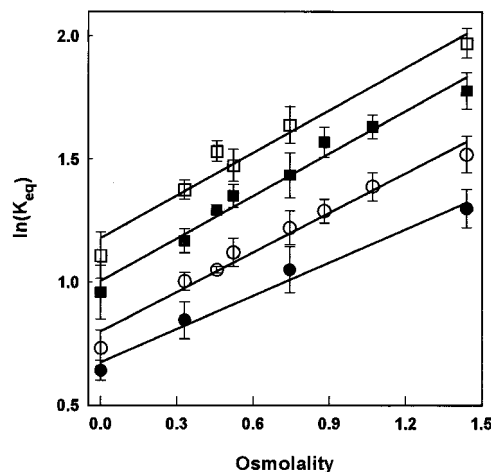


FIG. 7. Relationship between $\ln(K_{eq})$ and mOsm used to determine change hydration between the MI and MII conformations, according to Equation 2, for solutions containing 50 mM ethanol (●), 100 mM ethanol (○), 300 mM ethanol (■), and 500 mM ethanol (□). Values of osmolality do not include the osmotic contribution of ethanol. However, including the osmolality of ethanol would move each set of symbols uniformly to the right and would have no effect on the slopes of the correlation lines and hence would not alter the derived values of ΔN_w .

fractional contribution of the direct effect of ethanol on rhodopsin increases with osmotic stress. This suggests that osmotic stress enhances the ability of ethanol to act directly on rhodopsin in a way that favors MII formation. It is also observed that at each osmolality the nonbilayer contribution generally decreases with increasing ethanol concentration.

One of the proposed mechanisms for the effect of ethanol on receptors is a change in hydrogen-bonded water (1, 2). In the absence of ethanol, at 20 °C, an examination of the MI to MII conversion as a function of osmotic stress showed that MII formation results in the net release of 20 ± 1 water molecules. This number increased to 35 water molecules when corrected for bilayer effects (13). If ethanol perturbs the hydrogen bonding of water to either MI or MII, it should alter the number of water molecules released upon MII formation. The effect of ethanol on ΔN_w , the change in the number of water molecules in osmolyte-inaccessible regions, was assessed by analyzing $\ln(K_{eq})$ as a function of osmolality for each concentration of ethanol according to Equation 2 (10). The positive, linear cor-

relations in Fig. 7 demonstrate that ethanol has not altered the basic relationship between increased osmolality and increased MII formation that was observed in the absence of ethanol. The values of ΔN_w derived from the data in Fig. 7 are 25 ± 3 for 50 mM ethanol, 30 ± 3 for 100 mM ethanol, 31 ± 3 for 300 mM ethanol, and 33 ± 4 for 500 mM ethanol. In our earlier studies (13), adjusting $\Delta(\Delta G)$ for bilayer contributions yielded a corrected number of water molecules released upon MII formation. Since both ethanol and osmotic pressure are known to have opposing effects on bilayer acyl chain packing, adjusting $\Delta(\Delta G)$ for the effect of these agents on the bilayer will again yield corrected numbers of released water molecules. This correction was carried out using Equation 4, as described under "Experimental Procedures," and results in a net bilayer correction that makes $\Delta(\Delta G)$ more negative for all osmolalities and ethanol concentrations. This demonstrates that the acyl chain ordering due to increased osmolality outweighs the disordering effect of ethanol, resulting in a net inhibitory contribution of the bilayer to MII formation. Plotting the corrected values of $\ln(K_{eq})$ versus osmolality yields about 49 molecules released upon MII formation for all ethanol concentrations studied. Here, we see that the apparent variation in numbers of released water molecules as a function of ethanol concentration is a reflection of the mixed effect of osmotic pressure and ethanol on bilayer acyl packing and not an inherent property of the system. The increase in ΔN_w with added ethanol suggests that ethanol can influence a second population of loosely bound water molecules in MII. Ethanol may replace all or part of this second population of waters in the rhodopsin hydration sphere. This represents a direct effect of ethanol on MII formation, independent of its effect on the phospholipid bilayer. The direct effect of ethanol does not appear to be present in the absence of osmolyte.

The formation of MII is accompanied by an increase in hydrogen bonding of one or two internal water molecules (20); thus, it is unlikely that the pockets that release water molecules during the MI to MII transition are in the protein interior. The cytoplasmic surface of rhodopsin undergoes significant structural rearrangement between MI and MII, and this is the most likely region to undergo a net loss of water during this transition. The ability of ethanol to increase the number of released water molecules suggests that there are about 15 additional water molecules, which are hydrogen-bonded to the protein in the MI conformation but which may be susceptible to replacement by ethanol in the MII conformation. A conclusion of the present study is that ethanol contributes to an increased loss of water molecules for the MII conformation relative to the MI conformation.

Examination of the combined effects of ethanol and osmotic stress on both the MI-MII conformational equilibrium and phospholipid acyl chain packing makes it possible to distinguish between direct effects of ethanol on the receptor and those mediated by the membrane. Increased osmolality enhanced the ethanol-induced broadening of the DPH orientational probability distribution (Fig. 3) and the ethanol-induced increase of the parameter f_v (Fig. 4). These observations strongly suggest that a portion of ethanol's enhancement of MII formation is due to increased acyl chain disorder. Prior knowledge of how membrane physical properties are related to MII

formation shows that the changes in acyl chain packing are unable to account for all of enhancement of MII by ethanol under conditions of osmotic stress, as shown in Fig. 6. Ethanol increases the number of water molecules released during the MI to MII transition, suggesting that ethanol disrupts protein-water hydrogen bonds during the formation of MII. Thus, by simultaneously measuring changes both in the physical properties of the membrane bilayer and protein function, it was possible to distinguish direct effects of ethanol on the protein and effects of ethanol that are mediated by the membrane. It should be noted that at physiologically relevant ethanol concentrations and osmolalities comparable with human plasma, there is about a 2.8-fold enhancement of the effect of ethanol on MII formation. In addition, about 90% of this enhancement is derived from the effect of ethanol on acyl chain packing in the lipid bilayer. This type of analysis should provide further insight into the effects of drugs and other perturbations on receptors like rhodopsin, which have their agonist/antagonist binding site in a region of the protein, which is within the membrane.

REFERENCES

1. Eyring, H., Woodbury, J. W., and D'Arrigo, J. S. (1973) *Anesthesiology* **38**, 415-424
2. Klemm, W. R. (1998) *Alcohol* **15**, 249-267
3. Franks, F., and Mathias, S. (eds.) (1982) *Biophysics of Water*, John Wiley & Sons, Inc., New York
4. Timasheff, S. N. (1993) *Annu. Rev. Biophys. Biomol. Struct.* **22**, 67-97
5. Chiou, J.-S., Ma, S.-M., Kamaya, H., and Ueda, I. (1990) *Science* **248**, 583-585
6. Chiou, J.-S., Krishna, P. R., Kamaya, H., and Ueda, I. (1992) *Biochim. Biophys. Acta* **1110**, 225-233
7. Slater, S. J., Ho, C., Taddeo, F. J., Kelly, M. B., and Stubbs, C. D. (1993) *Biochemistry* **32**, 3714-3721
8. Mitchell, D. C., and Litman, B. J. (1994) *Biochemistry* **33**, 12752-12756
9. Mitchell, D. C., Lawrence, J. T. R., and Litman, B. J. (1996) *J. Biol. Chem.* **271**, 19033-19036
10. Parsegian, V. A., Rand, R. P., and Rau, D. C. (1995) *Methods Enzymol.* **259**, 43-94
11. Arakawa, T., and Timasheff, S. N. (1985) *Biochemistry* **24**, 6756-6762
12. Rand, R. P., Fuller, N. L., Butko, P., Francis, G., and Nicholls, P. (1993) *Biochemistry* **32**, 5925-5929
13. Mitchell, D. C., and Litman, B. J. (1999) *Biochemistry* **38**, 7617-7623
14. Yeagle, P. L., Alderfer, J. L., and Albert, A. D. (1997) *Biochemistry* **36**, 9649-9654
15. Schertler, G. F. X., and Hargrave, P. A. (1995) *Proc. Natl. Acad. Sci. U. S. A.* **92**, 11578-11582
16. Unger, V. M., Hargrave, P. A., Baldwin, J. M., and Schertler, G. F. X. (1997) *Nature* **389**, 203-206
17. Kibelbek, J., Mitchell, D. C., Beach, J. M., and Litman, B. J. (1991) *Biochemistry* **30**, 6761-6768
18. Mathews, R., Hubbard, R., Brown, P., and Wald, G. (1963) *J. Gen. Physiol.* **47**, 215-222
19. Litman, B. J., and Mitchell, D. C. (1996) in *Biomembranes* (Lee, A., ed) Vol. 2A, pp. 1-32, JAI Press, Greenwich, CT
20. Rath, P., Delange, F., DeGrip, W. J., and Rothschild, K. J. (1998) *Biochem. J.* **329**, 713-717
21. Maeda, A., Ohkita, Y. J., Sasaki, J., Shichida, Y., and Yoshizawa, T. (1993) *Biochemistry* **32**, 12033-12038
22. Mitchell, D. C., Straume, M., Miller, J. L., and Litman, B. J. (1990) *Biochemistry* **29**, 9143-9149
23. Mitchell, D. C., Straume, M., and Litman, B. J. (1992) *Biochemistry* **31**, 662-670
24. Litman, B. J., and Mitchell, D. C. (1996) *Lipids* **31**, (suppl.) 193
25. Miller, K. W. (1985) *Int. Rev. Neurobiol.* **270**, 1-61
26. Lehtonen, J. Y. A., and Kinnunen, K. J. (1994) *Biophys. J.* **66**, 1981-1990
27. Smith, H. G., and Litman, B. J. (1982) *Methods Enzymol.* **81**, 57-61
28. Straume, M., Mitchell, D. C., Miller, J. L., and Litman, B. J. (1990) *Biochemistry* **29**, 9135-9142
29. Mitchell, D. C., and Litman, B. J. (1998) *Biophys. J.* **74**, 879-891
30. Straume, M., and Litman, B. J. (1987) *Biochemistry* **26**, 5113-5120
31. Johnson, M. L., and Frasier, S. G. (1985) *Methods Enzymol.* **117**, 301-342
32. Deitrich, R. A., and Harris, R. A. (1996) *Alcohol Clin. Exp. Res.* **20**, 1-2
33. Barry, J. A., and Gawrisch, K. (1994) *Biochemistry* 8082-8088